

Equation (46) then yields

$$\langle v \rangle = D[(\partial \ln D / \partial x) - (\partial \ln \gamma / \partial x) + 2d^{-1}B], \quad (62)$$

and with Eq. (15), we find

$$J = -D(1 + \partial \ln \gamma / \partial \ln c)(\partial c / \partial x) + 2cDd^{-1}B. \quad (63)$$

These equations agree with Eqs. (55)–(57) since

$$\langle v_f \rangle = -D(\partial \ln \gamma / \partial x) + 2Dd^{-1}B. \quad (64)$$

Also they agree with equations found in Ref. 1. In this reference, estimates of B also are given, and explicit equations for $\langle v \rangle$ and J are found.

VII. DISCUSSION

The explicit expressions for J and $\langle v \rangle$ in terms of A and B as given in Eqs. (55)–(57) are two very useful results. They apply not only when there are chemical-concentration gradients but also when there are other

forces, such as those from a temperature gradient or an electric field. In addition, an explicit expression (Eq. 25) for the correlation factor regardless of gradients or driving forces was obtained. The derivation of this expression depended directly on the introduction of N , the effective number of independent jumps.

Although the notation at times is rather involved, the present treatment presents final expressions for D , f , J , and $\langle v \rangle$ in a rather simple form. These expressions are correct to first order in small quantities. Since the correlation factor is completely contained in the expression for the effective jump frequency itself, each effective jump is independent of the previous path of the atom. This allows the actual complex motion of the atom for a three-dimensional correlated walk to be expressed in terms of a one-dimensional random walk. Also it leads to the not-so-obvious conclusion that the same correlation factor f appears in the expression for $\langle X \rangle$ as for $\langle X^2 \rangle$.

Nuclear Resonance Study of Hyperfine Fields in Nickel-Rich Nickel-Cobalt Alloys

R. L. STREEVER AND G. A. URIANO

National Bureau of Standards, Washington, D. C.

(Received 1 September 1964; revised manuscript received 11 January 1965)

The nuclear-magnetic-resonance line shapes of ^{59}Co and ^{61}Ni have been studied in Ni-Co alloy powders, using the free-precession method, by plotting the amplitude of the spin-echo signal across the inhomogeneously broadened lines. The ^{59}Co nuclear resonance has been studied in the concentration range from 1 to 41.2 at. % cobalt and the ^{61}Ni from 1 to 14.8% cobalt. Both ^{61}Ni and ^{59}Co resonance frequencies increase roughly linearly with increasing cobalt concentration. The higher concentration ^{59}Co studies were made at 77°K, while the low-concentration ^{59}Co studies and the ^{61}Ni studies were made at 4°K. Well-resolved satellite structure is observed. A line is observed approximately 10 MHz above the resonance frequency appropriate to dilute ^{59}Co in nickel. This line is believed due to cobalt atoms with one cobalt neighbor in the nearest-neighbor shell. A similar line is observed in the ^{61}Ni case approximately 5 MHz above the pure-nickel resonance frequency. A discussion of the relation between hyperfine fields and local atomic moments is made, and it is concluded that the conduction-electron polarization is a major contribution to the hyperfine fields in these alloys. An oscillatory variation of the spin density about the solute atoms is indicated and appears to explain the observed spectra.

I. INTRODUCTION

HYPERFINE field studies in the Ni-Co alloy system are interesting because the system is typical of the binary ferromagnetic alloys. Hyperfine fields in these ferromagnetic materials have been studied by several people.^{1–3} Contributions to the hyperfine field at the nuclei in these alloys arise from the polarization of inner core electrons of the parent atom by the unpaired d electrons on the atom, from the interaction

between the nuclear spin and the unquenched orbital angular momentum of the parent atom, and from the polarization of the conduction electrons. Thus, the correlation of the hyperfine fields with local $3d$ atomic moments in these materials provides information about the conduction-electron polarization.

The cobalt hyperfine field has been previously determined in pure cobalt and in a 60-40% Ni (all percentages are atomic) alloy by specific-heat measurements.⁴ The ^{59}Co nuclear resonance has also been studied in pure cobalt⁵ and with small percentages of cobalt in

¹ W. Marshall, Phys. Rev. **110**, 1280 (1958).

² W. Marshall and C. E. Johnson, in *Metallic Solid Solutions, A Symposium on their Electronic and Atomic Structure*, edited by J. Friedel and A. Guinier (W. A. Benjamin Inc., New York, 1963).

³ R. E. Watson and A. J. Freeman, Phys. Rev. **123**, 2027 (1961).

⁴ V. Arp, D. Edmonds, and R. Petersen, Phys. Rev. Letters **3**, 212 (1959).

⁵ A. M. Portis and A. C. Gossard, J. Appl. Phys. **31**, 205S (1960).

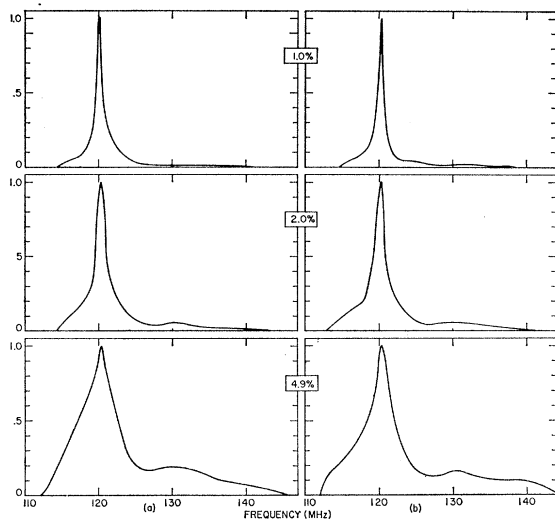


FIG. 1. The ^{59}Co line shapes at 4°K for low concentrations, corrected, as discussed in text. (a) Low rf level; (b) high rf level.

nickel^{6,7} by nuclear resonance. The ^{61}Ni nuclear resonance has been studied in pure nickel⁸ and with small percentages of nickel in cobalt.⁹ In this work we have used the free-precession method to study the ^{59}Co and ^{61}Ni nuclear resonances in the nickel-rich nickel-cobalt alloys. The ^{59}Co nuclear resonance has been studied in the concentration range from 1 to 41.2% cobalt, while the ^{61}Ni resonance has been studied in the concentration range from 1 to 14.8% cobalt. We have determined the shape of the inhomogeneously broadened resonance lines in these alloys by measuring the amplitude of the spin-echo signal as a function of the frequency across the lines. The studies are particularly interesting in the dilute alloys, as we have been able to resolve lines from nuclei with various nearest-neighbor environments. In Sec. II the experimental methods are discussed, and in Sec. III the results are presented. In Sec. IV, in addition to a discussion of the satellite structure of the resonance lines at low concentrations of cobalt, a general discussion of the hyperfine fields in the alloy system is given and a correlation is made with the local $3d$ atomic moments measured by neutron diffraction.

II. EXPERIMENTAL

A. Samples

The samples used in this work were prepared by induction heating of the appropriate amounts of cobalt

⁶ L. H. Bennett and R. L. Streever, *J. Appl. Phys.* **33**, 1093S (1962).

⁷ R. C. La Force, S. F. Ravitz, and G. F. Day, *Proceedings of the International Conference on Magnetism and Crystallography* (The Physical Society of Japan, Bunkyo-ku-Tokyo, 1962) and *J. Phys. Soc. Japan Suppl.* **17**, 99 (1962).

⁸ L. H. Bruner, J. I. Budnick, and R. J. Blume, *Phys. Rev.* **121**, 83 (1961).

⁹ R. L. Streever, L. H. Bennett, R. C. La Force, and G. F. Day, *Phys. Rev.* **128**, 1632 (1962).

and nickel. The alloys in the concentration range 1–14.8% cobalt were sprayed into fine particles $10\ \mu$ or smaller. They were then annealed for 1 h at 1000°C under a hydrogen atmosphere. The alloys from 25.7 to 41.2%, were cast into ingots and then filed into fine particles $50\ \mu$ or smaller. These samples were then studied as filed.

B. Equipment

The nuclear resonances were studied using the free-precession method. An Arenberg Ultrasonics Laboratory (AUL) pulsed oscillator (AUL 650-C) was used to supply the rf pulses. A separate receiving coil of one or two turns was wound around the transmitting coil. For the ^{61}Ni studies a preamplifier (AUL 620) was connected through a $50\text{-}\Omega$ cable to the receiving coil. The preamplifier was followed by a wide-band amplifier (AUL 600-C) and detector. The spin echo was observed on an oscilloscope. For the ^{59}Co studies a television tuner (Standard Kollsman, GK-2550) was used to convert the rf signal down to about 20 MHz before it was passed through the amplification-detection system. It was necessary to match the pickup coil to the TV tuner in order to avoid transmission-line problems which occurred at the higher frequencies. This was accomplished by placing a $300\text{-}\Omega$ resistor across the pickup coil, which was then connected with $300\text{-}\Omega$ TV antenna wire to the $300\text{-}\Omega$ input of the TV tuner. This enabled the tuning of the pulsed oscillator to be independent of the TV tuner, and resulted in a detection system with essentially a constant gain at any frequency.

All studies were made at low temperatures. The ^{59}Co studies were made at 77°K , and the concentrations below 6.8% were also studied at 4°K for improved sensitivity. All nickel studies were made at 4°K . The 4°K studies were made using exposed-tip helium Dewars. The finger of the Dewar fitted inside the pulsed-oscillator transmitting coil. The outside of the inner finger of the Dewar was coated with platinum to reduce helium loss and scribed in order to allow rf field penetration. The alloy powder was sealed off in glass tubes (under a helium-gas atmosphere for the 4°K measurements) and placed inside the inner finger of the Dewar. For the ^{61}Ni studies the sample tube was about 15 mm in diameter, while the coil diameter was about 27 mm. For the ^{59}Co studies a Dewar with a smaller finger was used. The sample diameter was about 10 mm and the coil diameter 19 mm.

The nuclear signal was calibrated by means of a VHF signal generator which was inductively coupled by means of a one-turn coil to the pickup coil. A special $50\text{-}\Omega$ cable and switch was used to connect the VHF signal generator to either a frequency counter or the calibration coil. A $50\text{-}\Omega$ terminator on this switch-cable combination ensured that the VHF signal generator saw a $50\text{-}\Omega$ impedance independent of frequency. When terminated in this manner, the VHF signal generator

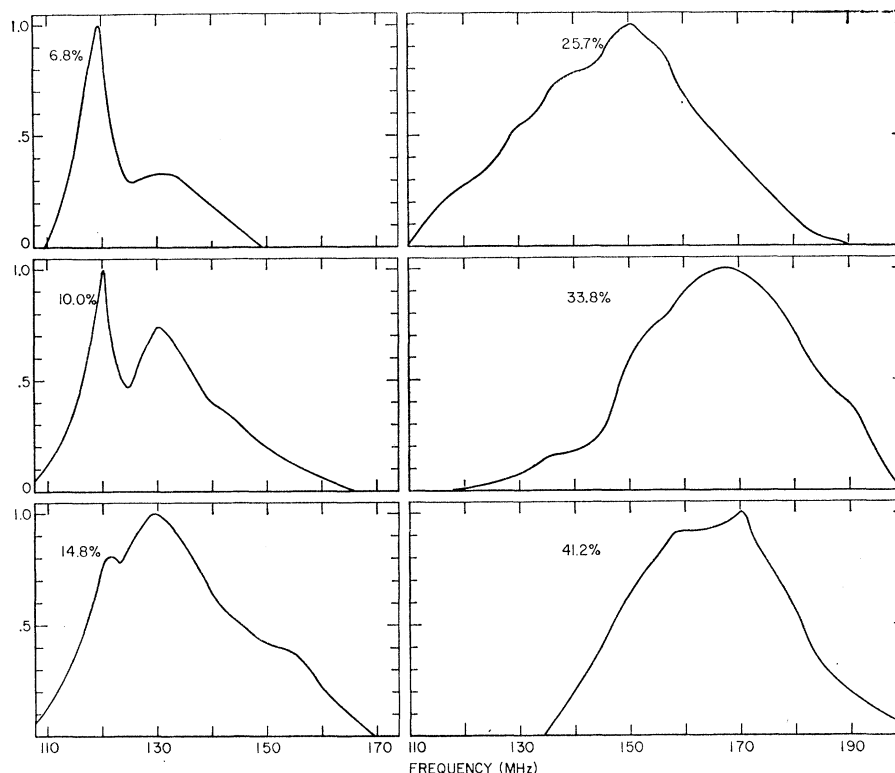


FIG. 2. Corrected ^{59}Co line shapes at 77°K for the higher concentrations, using high rf level.

put out a calibration voltage independent of frequency. The calibration voltage accuracy was $\pm 10\%$.

C. Measurements

All measurements were made in zero applied field. If one studies the behavior of the nuclear spin-echo signal following two rf pulses as a function of rf pulse level (keeping the pulse width and separation fixed), one finds that the echo signal rises sharply at low rf pulse levels. It reaches a maximum at a relatively low rf level and slowly decreases as the rf level is further increased.¹⁰ The signals at low rf levels are mainly from nuclei in domain walls, while the high rf signals are mainly from nuclei in domains. At the lower concentrations the resonances were studied at both high and low rf pulse levels. In making the low rf level measurements, the pulse amplitude was adjusted to the echo maximum at each point in the line, while the pulse widths and separation were kept fixed. The pulse widths were made approximately equal, since in a ferromagnetic metal, as a result of the skin depth and the distribution in enhancement factors, the 90° and 180° condition is never satisfied for all the nuclei.

For the broader lines (greater than 2 MHz) the pulse width was left at its minimum value of $1 \mu\text{sec}$, while for narrower lines broader pulses were used. (For best reproduction of the line shape, the criterion is that the

distribution in frequencies within the pulse should be less than the line width so that only a portion of the inhomogeneously broadened line is excited at each point across the line.) The pulse separation was kept small enough so that the echo decay due to T_2 was negligible. For the ^{59}Co in nickel, T_2 at 77° and low concentrations varied from 40 to $180 \mu\text{sec}$,¹¹ depending on the rf level, and was longer at 4°K , so that a typical pulse separation was about $20 \mu\text{sec}$. The T_2 in pure nickel at 4°K is 15–25 msec,¹² depending on the rf level, so that the pulse separation used for the ^{61}Ni studies was about 0.3 msec. After adjusting the pulsed oscillator to a particular frequency and adjusting the rf to an echo maximum, the preamplifier was tuned to a maximum echo signal. The calibrator signal was then turned on and heterodyned with the nuclear signal, and the frequency was measured by switching the calibrator signal into a counter. A 1000-Hz modulation was then put on the calibrator signal, and the amplitude of the calibrator signal was made equal to the amplitude of the echo, both being observed on the oscilloscope. The calibrator signal voltage was then taken as the amplitude of the nuclear signal at that frequency. The high-rf studies were made in a similar fashion, except that the rf was kept at the maximum value that could be obtained with the pulsed oscillator. The maximum rf level was

¹¹ R. L. Streever, Phys. Rev. **134**, A1612 (1964).

¹⁰ M. Weger, thesis, University of California at Berkeley, 1961 (unpublished).

¹² M. Weger, E. L. Hahn, and A. M. Portis, J. Appl. Phys. **32**, 124S (1961).

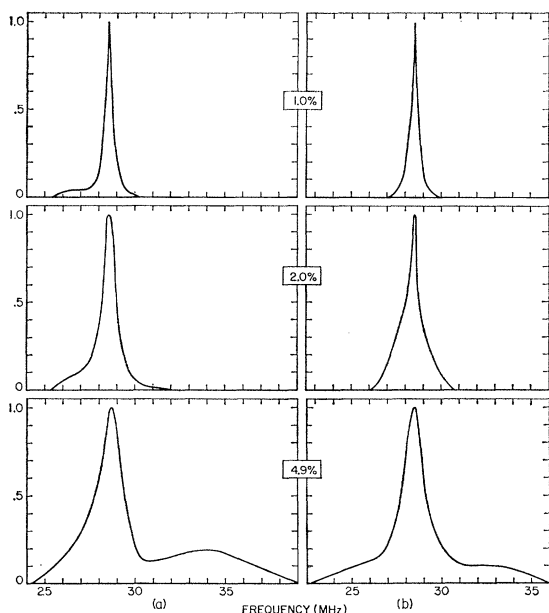


FIG. 3. Corrected ^{61}Ni line shapes at 4°K for low concentrations. (a) Low rf level; (b) high rf level.

about 300 V peak to peak, corresponding to a field of about 0.5 mT ($1 \text{ T} = 10^4 \text{ G}$).

The spin-echo signal observed in a free-precession experiment is proportional to the macroscopic moment M . Since this is proportional to the microscopic nuclear moment times the polarization, we have divided the experimentally obtained echo intensities at each frequency by that frequency to take into account the additional nuclear polarization at higher frequencies. As long as one keeps adjusting the rf level to an echo maximum or works at higher rf levels where the echo signal is not a strong function of the rf level, it is probably not necessary to correct for the changing rf enhancement across the resonance line.

III. RESULTS

The results of the ^{59}Co studies for the concentration 4.9% and below are shown in Fig. 1. These concentrations were studied at 4°K at both low rf levels (at the echo maximum) and high rf levels. The low rf signals were from nuclei in domain walls, while the high rf signals were mainly from nuclei in the domains. The higher concentration samples were studied only at high rf levels and at 77°K , and the results are shown in Fig. 2. The signals in these samples are believed to be mainly from nuclei in the domains. The samples were all annealed except for the concentrations 25.7% and above, which were studied as filed. The curves shown are all corrected for the increased polarization at higher frequencies, as discussed previously.

All of the ^{61}Ni studies were made at 4°K to compensate for the weaker signal. The low-concentration studies, shown in Fig. 3, were made at both high and

low rf levels in annealed samples. The concentrations above 4.9% were studied only at high rf levels and the results are shown in Fig. 4. The ^{61}Ni studies in the 6.8, 10.0, and 14.8% samples were made in unannealed powders (as produced by the spraying process). The reasons for this were two. First, at the higher concentrations the nickel signal was relatively weak, and the signal from the unannealed samples appeared somewhat stronger than that from the annealed ones. This may perhaps be due to the larger skin depth in the unannealed samples. Also, we observed in the well-annealed

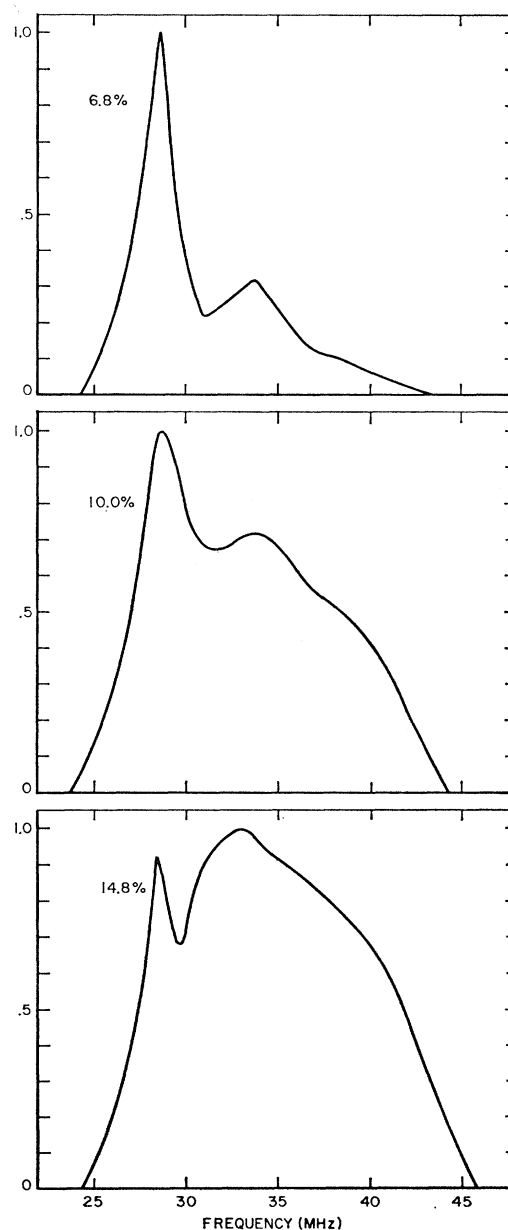


FIG. 4. Corrected ^{61}Ni line shapes at 4°K for higher concentrations, using high rf level.

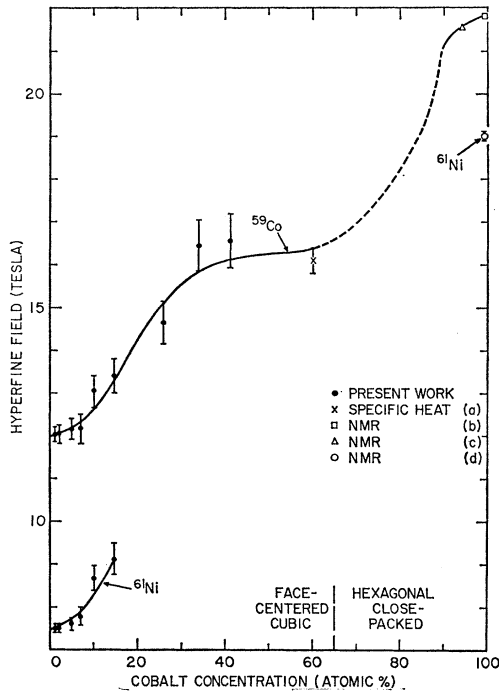


FIG. 5. A plot of hyperfine field in tesla (one T = 10^4 G) versus cobalt concentration in atomic percent. Fields have been extrapolated to 0°K. All the hyperfine fields are negative with respect to the net magnetization (see text). (a) Reference 4; (b) Ref. 5; (c) Ref. 13; (d) Ref. 9.

samples a strong resonance whose behavior was considerably different from the nuclear resonance. This resonance may be associated with electronic losses, possibly due to domain-wall motion. This resonance was considerably weaker in the unannealed samples. Unlike the nuclear signal, which went through a maximum at low rf levels, the “electronic” signal continued to increase at as high an rf pulse level as could be obtained. Furthermore, the “electronic” signal had a relatively short T_2 (in the μsec region) and extended over 40 MHz or more. Because of the much shorter T_2 of the “electronic” signal, the best way to discriminate against it was to keep the separation of the exciting pulses relatively large. Above 5 at.%, little or no difference in line shape was found between annealed and unannealed samples.

In Fig. 5 we have plotted the hyperfine fields obtained from the centers of gravity of the curves of Figs. 1–4. The ^{59}Co data at 77°K have been extrapolated to 0°K by knowing the difference in frequency of 1% ^{59}Co in nickel at 77 and 0°K (about 300 kHz) and the same difference for ^{59}Co in pure cobalt (also about 300 kHz). We have included the ^{59}Co hyperfine field for the 60–40% Ni alloy, as determined by specific-heat measurements.⁴ Also shown are the ^{59}Co hyperfine field in pure cobalt,⁵ the ^{59}Co field for cobalt with 7% nickel,¹³ and

¹³ Y. Koi, A. Tsujimura, T. Hihara, and T. Kushida, J. Phys. Soc. Japan **16**, 574 (1961).

the field for 1% ^{61}Ni in cobalt.⁹ These were determined by nuclear magnetic resonance. These values have been extrapolated to 0°K by assuming the same temperature dependence of frequency as in pure cobalt. In calculating the hyperfine fields, the values of the nuclear moments were taken to be 4.583 nm¹⁴ for that of ^{59}Co and 0.746 nm¹⁵ for that of ^{61}Ni . The nuclear hyperfine fields are negative (i.e., opposed to the electronic magnetization direction) in pure cobalt¹² and pure nickel.¹⁶ Therefore, as can be seen from Fig. 5, they are negative across the whole alloy system for both nickel and cobalt.

IV. DISCUSSION

A. General Discussion of Hyperfine Fields

Before discussing the detailed hyperfine field distribution, we will give a general discussion of the hyperfine fields and their relation to the local $3d$ atomic moments in this system. For a system like Ni-Co, which lies on the main linear portion of the Slater-Pauling curve, the theory of Friedel¹⁷ predicts that the individual atomic moments should be unchanged on alloying and should be essentially equal to the pure-metal values. The theory assumes that the excess nuclear charge is screened out at the impurity-atom site alone, so that the d moments remain essentially equal to their values in the pure metals and are localized at the atomic sites. Collins and Wheeler¹⁸ have used neutron-diffraction techniques to study the magnetic-moment distributions in the Ni-Co alloy system. Within their experimental errors the magnetic moments remain essentially unchanged over the whole alloy system and are $\mu_{\text{Ni}}=0.6$ and $\mu_{\text{Co}}=1.7$ in units of the Bohr magneton.

We try to fit the hyperfine fields at both cobalt and nickel in this system to an expression of the form

$$H_A(c) = a\mu_A + b\bar{\mu}(c). \quad (1)$$

Here H_A is the hyperfine field at atom A , μ_A is the moment of atom A , and $\bar{\mu}(c)$ is the average moment of the alloy.

$\bar{\mu} = c\mu_{\text{Co}} + (1-c)\mu_{\text{Ni}}$, where c is the fractional concentration of cobalt. Taking $\mu_{\text{Ni}}=0.6$ and $\mu_{\text{Co}}=1.7$, the expression

$$H_{\text{Co}} = -4.0\mu_{\text{Co}} - 8.8\bar{\mu}(c) \quad (2)$$

gives the experimental hyperfine field in teslas at 0°K for cobalt in pure cobalt (–21.8 T) and for cobalt in nickel (–12.1 T). A similar expression for nickel with the same constants a and b

$$H_{\text{Ni}} = -4.0\mu_{\text{Ni}} - 8.8\bar{\mu} \quad (3)$$

¹⁴ R. Freeman, G. R. Murray, and R. E. Richards, Proc. Roy. Soc. (London) **242**, 455 (1957).

¹⁵ P. R. Locher and S. Geschwind, Phys. Rev. Letters **11**, 333 (1963).

¹⁶ H. F. Horst and R. F. Obenshain, Z. Physik **163**, 17 (1961).

¹⁷ J. Friedel, Nuovo Cimento Suppl. **7**, 287 (1958).

¹⁸ M. F. Collins and D. A. Wheeler, Proc. Phys. Soc. (London) **82**, 633 (1963).

gives the field in pure nickel (-7.7 T) and nickel in cobalt (-17.4 T). This compares with the experimental values (at 0°K) of -7.5 T and -19.0 T. The fact that Eqs. (2) and (3) give approximately the hyperfine fields in this system over the entire concentration range shows that the hyperfine fields can be given approximately by an expression which contains a term proportional to the local moment of the parent atom plus a term proportional to the average moment.

It is interesting that these equations also give approximately the correct value for the hyperfine field of copper in nickel. The nuclear hyperfine fields for both copper and nickel in Cu-Ni alloys have been studied by Asayama and co-workers.^{19,20} They point out¹⁹ that their results can best be understood by assuming that copper itself carries no moment. Then using Eq. (1) with the same constants and assuming $\mu_A = 0$ and $\bar{\mu} = 0.6$ one obtains a field of -5.3 T at the copper nucleus for a small amount of copper in nickel. This is close to their experimental value at 0°K of -5.0 T.

Equation (1) appears to provide a phenomenological correlation of the hyperfine fields with the local $3d$ moments in these alloys. The first term in Eq. (1) represents the contributions to the hyperfine field from the spin of the parent atom. These contributions have been discussed by various people¹⁻³ and include the core-polarization contribution, the contribution from the unquenched orbital angular momentum and the contribution from the conduction-electron polarization. All of these contributions would be expected to be proportional to μ_A . The second term in Eq. (1) which is proportional to $\bar{\mu}$ would be zero for a magnetic atom in a nonmagnetic host and represents the contribution to the hyperfine field from neighboring atoms. If we assume this term is due to conduction-electron polarization, then the conduction-electron polarization by neighboring atoms must be negative.

The polarization of the conduction electrons by the s - d exchange has been discussed recently by Overhauser and Stearns.^{21,22} For the case of iron, the s - d exchange results in a positive conduction-electron polarization at any given iron atom due to its own spin, but this is largely cancelled in pure iron by a negative polarization arising from all the neighboring iron atoms. A similar mechanism in the Ni alloys would account for the negative contribution from neighboring atoms. Anderson²³ and Clogston and Anderson²⁴ have also discussed the conduction-electron polarization resulting from s - d mixing, and have shown that the positive contribution is largely cancelled out by a negative conduction-electron polariza-

tion arising from a shift in energy levels of the conduction bands according to a compensation theorem. Both s - d mixing and s - d exchange may be important. In any case, the close proportionality of hyperfine fields to local moments in the pure metals, and the fact that the core-polarization and orbital contributions approximately account for the observed hyperfine fields in the pure metals, suggest that positive and negative contributions to the conduction-electron polarization tend to cancel out in the pure metals and the net conduction-electron polarization at any nucleus is nearly zero.

It is interesting to pursue this idea further. Taking the case of cobalt we can rewrite Eq. (2) as follows:

$$H_{\text{Co}}(c) = -12.8\mu_{\text{Co}} + 8.8[\mu_{\text{Co}} - \bar{\mu}(c)]. \quad (4)$$

The second term, which is zero in pure cobalt, may represent the positive and negative conduction-electron polarizations. This would leave a contribution of -12.8 T/ μ_B , which would be due to the core polarizations and orbital terms. This is reasonable since the theoretical core polarization might be about -16.0 T/ μ_B (Ref. 3), while the orbital contribution might be about $+3.0$ T/ μ_B (Ref. 2). For cobalt in nickel the second term in Eq. (4) would be positive, suggesting that the sign of the net conduction-electron polarization at the solute atom in question in the dilute alloy may depend on whether its moment is greater than or less than the average moment.

B. Detailed Discussion

A detailed interpretation of these spectra is difficult, but we propose the following one. Consider the ^{59}Co results of Fig. 1 (note that there is relatively little difference between the low and high rf-level results), and also the high-concentration results of Fig. 2. The broad line at 130 MHz we attribute to ^{59}Co atoms with one cobalt atom in the nearest-neighbor shell. We have measured the *integrated* intensity of this line compared with the total *integrated* intensity and have found it to be consistent at each concentration with this assumption. The effects of neighbors in more distant shells are then assumed to give rise to broadening and structure around 120 MHz. In fact, the spectra at every concentration can be understood if we assume that the effect of each cobalt in the nearest-neighbor shell is to increase the frequency by ≈ 10 MHz, so that lines due to 1, 2, 3 cobalt neighbors appear at ≈ 130 MHz, 140 MHz, 150 MHz, etc. By 25% Co the effects of neighbors in second and third shells appear to have broadened the 120 MHz line sufficiently that all the lines due to various numbers of nearest neighbors are of approximately the same width, and the intensities of these lines go simply as the statistical probability. At 25% the 3-neighbor line should be at a maximum, as observed. On this model, the pure Co frequency will be 120 MHz above that for Co in Ni, or 240 MHz. This is in reasonable accord with the actual frequency, considering that the linear effect

¹⁹ K. Asayama *et al.*, J. Phys. Soc. Japan **18**, 458 (1963).

²⁰ K. Asayama, J. Phys. Soc. Japan **18**, 1727 (1963).

²¹ M. B. Stearns and S. S. Wilson, Phys. Rev. Letters **13**, 313 (1964).

²² A. W. Overhauser and M. B. Stearns, Phys. Rev. Letters **13**, 316 (1964).

²³ P. W. Anderson, Phys. Rev. **124**, 41 (1961).

²⁴ A. M. Clogston and P. W. Anderson, Bull. Am. Phys. Soc. **6**, 124 (1961).

of nearest neighbors probably does not hold over the whole range.

The broadening of the 130-MHz line, even at low concentrations, is probably due to the effects of anisotropy in the shifts produced by the neighbors. For a unique magnetization direction (determined by crystal anisotropy) we would expect the anisotropy to give rise to a splitting²⁵ where actually a broadening is observed. The broadening at low powers may be due to the fact that a rather broad region of the wall is excited and the spins turn in going across the wall. Even at the wall center or in domains the shift anisotropy will lead to a broadening if the magnetization direction is not determined by the crystal anisotropy, but is determined by the directions of domains of closure at the particle surface²⁶ (the skin depth in these powders is comparable to the dimensions of the domains of closure at the surface). This probably explains why the spectra at high and low rf powers are not appreciably different.

The effects of second and third neighbors, although small, are not necessarily negligible. The partially resolved line at 117 MHz has about the right integrated intensity to be due to cobalt atoms with one cobalt in the second-neighbor shell (and none in the first). The third-neighbor shell shift must be close to zero, perhaps ≈ 0.2 MHz higher in frequency.

The ⁶¹Ni results appear to be similar to the ⁵⁹Co results. The line appearing at 34 MHz corresponds to the ⁵⁹Co line at 130 MHz, while the line at 27 MHz corresponds to the ⁵⁹Co line at 117 MHz.

The spatial variation of the 4s spin density away from the solute atom may be similar to that discussed for iron by Overhauser and Stearns,²² the Co acting as a positive excess moment in the Ni lattice. From Eq. (4) of the preceding section and the accompanying discussion, we estimate the net conduction-electron polarization field at ⁵⁹Co for dilute Co in Ni relative to the nickel to be about +9.7 T. The field shifts at cobalt nuclei in first- and second-neighbor shells to the cobalt atom are, from our assignments of the satellite lines, -1.0 and 0.3 T, while the shifts at nickel nuclei are -1.5 and 0.4 T. The field shift at the third-neighbor shell appears to be close to zero, perhaps slightly negative. Therefore, the spin density must oscillate in going out from the solute atom.

Since the number of conduction electrons per atom for Ni should be ≈ 0.4 , we might expect k_F for nickel to be $\approx 1 \times 10^{18}$ cm⁻¹, which is close to the value for iron. The first-, second-, and third-neighbor distances in nickel are 2.5 Å, 3.5 Å, and 4.3 Å, corresponding to $2k_F R$ of 5.0, 7.0, and 8.6. Consequently, a shift at the

nearest-neighbor shell of the opposite sign to that at the central atom, a shift at the second-neighbor shell of the same sign as that at the central atom, and a shift close to zero for the third shell is reasonable (see Fig. 2 of Ref. 22).

V. CONCLUSIONS

In addition to the contribution to the hyperfine field from the parent atom, there is found to be a large contribution from neighboring atoms. Assuming the contribution from neighboring atoms to arise from conduction-electron polarization, the polarization induced by any given atom at a nearest neighboring atom must be negative (with respect to the 3d spin). The spatial variation of the 4s spin density appears to be similar to that observed in iron.^{21,22}

Note added in proof. Mary Beth Stearns has done a computer analysis of our experimental ⁵⁹Co resonance spectra at several concentrations using a method similar to that described in Ref. 21. Details of the analysis will be published later. She assumed that the resonance spectra is composed of a series of elementary lines; each elementary line being due to a different nearest-neighbor configuration. Nearest-neighbor contributions to the resonance spectra were considered up to the fifth-nearest-neighbor shell. Each statistically significant component was assigned a shift and width appropriate to the 1% alloy (about 1 MHz for the ⁵⁹Co case). Additivity of effects from atoms in the same neighbor shell was also assumed. She found a reasonably good fit to the 2% ⁵⁹Co in nickel spectra by taking the shift due to one ⁵⁹Co atom in the nearest-neighbor shell to be -3 MHz or -3% of the hyperfine field at the ⁵⁹Co nuclei in the 1% sample. The shift due to one ⁵⁹Co atom in the second nearest-neighbor shell was found to be +10 MHz or +9% of the hyperfine field at the ⁵⁹Co nuclei in the 1% sample. Smaller but finite shifts from the more distant neighbor shells were also found. Approximately the same shift assignments gave a good fit to the 5 and 7% ⁵⁹Co in nickel spectra. Her results indicate that the line occurring at about 130 MHz at low concentrations is mainly due to the ⁵⁹Co atom in the second nearest-neighbor shell while the partially resolved line at 117 MHz is mainly due to one ⁵⁹Co atom in the nearest-neighbor shell. Similar considerations should apply to the ⁶¹Ni case. Consequently it appears that our detailed interpretation proposed in Sec. IV B may be in error.

ACKNOWLEDGMENTS

We would like to thank D. E. Brown for technical assistance and would also like to thank the International Nickel Company for preparing the higher concentration Ni-Co ingots.

²⁵ A. M. Portis and J. Kanamori, J. Phys. Soc. Japan **17**, 587 (1962).

²⁶ J. Friedel and P. de Gennes, Compt. Rend. **251**, 1283 (1960).